

Cosmological signature and light Dark Matter in Dirac $L_\mu - L_\tau$ model

Pritam Das^{*}

Department of Physics, Salbari College, Baksa, Assam-781318, India

Abstract

We revisit an anomaly-free extension of the Standard Model (SM) *viz.* gauged $L_\mu - L_\tau$ model in the Dirac framework, where the local $U(1)_{L_\mu - L_\tau}$ symmetry breaks and gives rise to a new gauge boson Z' and corresponding gauge coupling $g_{\mu\tau}$. Three additional heavy vector-like fermions, three light right-handed neutrinos and two heavy singlet scalars are added to complete the model framework for Dirac neutrinos. Another singlet vector-like fermion is added with a new gauge charge, which serves as a viable DM candidate, and the correct relic abundance is obtained via the resonance effect. The parameter space is considered after satisfying the current bounds on $M_{Z'}$ and the gauge coupling $g_{\mu\tau}$. The influence of dark radiations coming from the additional light degrees of freedoms are studied in connection with the dark matter. After imposing all relevant theoretical and experimental constraints, the allowed parameter space is found to be highly restricted yet still accessible to ongoing and near-future experiments, rendering the scenario strongly predictive. Moreover, clear correlations among the relevant observables emerge throughout this study, making the model testable in current and future experimental searches.

^{*}Electronic address: prtmdas9@gmail.com

I. INTRODUCTION

The experimental discovery of neutrino mass demands beyond the Standard Model (BSM) frameworks. However, the exact nature of them is still an enigma as to whether they are *Dirac* or *Majorana*? The essential difference lies in the fact that in the Dirac scenario, there are a minimum of two more light degrees of freedom (DOF) known as right-handed neutrinos (ν_R) than in the Majorana scenarios. The presence of additional light DOF contributes to the effective relativistic DOF, ΔN_{eff} . The SM prediction $N_{\text{eff}} = 3.045$ [1–3], is consistent with the current Planck 2018 measurement, $N_{\text{eff}} = 2.99 \pm 0.17$ [4]. A similar bound also exists from big bang nucleosynthesis (BBN) $2.3 < N_{\text{eff}} < 3.4$ at 95% CL [5]. Future experiments like CMB Stage IV (CMB-S4) is expected to reach an unprecedented sensitivity of $\Delta N_{\text{eff}} = N_{\text{eff}} - N_{\text{eff}}^{\text{SM}} = \pm 0.06$ [6], taking it closer to the SM prediction. Enhancements of ΔN_{eff} in Dirac neutrino models have been studied in several recent works [7–21]

Due to the superlight nature and weak interaction strength, ν_R decouples early, influencing the effective relativistic degrees of freedom. If ν_R are in thermal equilibrium and they decouple at temperature $T_{\nu_R}^{\text{dec}}$, then the change in the effective numbers of neutrino species with the standard value $N_{\text{eff}}^{\text{SM}}$ can be expressed as [1, 12]:

$$\Delta N_{\text{eff}} = N_{\text{eff}} - N_{\text{eff}}^{\text{SM}} = N_{\nu_R} \left[\frac{g_*(T_{\nu_L}^{\text{dec}})}{g_*(T_{\nu_R}^{\text{dec}})} \right]^{4/3}, \quad (1)$$

where, N_{ν_R} is number of RH neutrino species.

The anomalous magnetic moments of leptons, especially those of the muon and electron, are also important for the SM. It has been a long-term test of the SM and has put strict limits on BSM theories. The anomalous magnetic moment of leptons has garnered significant attention in the literature, as it contests the phenomenological efficacy of the Standard Model. The Fermilab Muon $g - 2$ experiment has released its final and most precise measurement of the muon anomalous magnetic moment, with a world-average value $a_{\mu}^{\text{Exp}} = 116592071.5(14.5) \times 10^{-11}$ at ~ 124 ppb precision [22], which sets a new benchmark for this quantity. This result is consistent, within current theoretical uncertainties, with recent Standard Model evaluations such as $a_{\mu}^{\text{SM}} = 116592033(62) \times 10^{-11}$ [23], while further improvements in the precision of the Standard Model prediction are needed to draw a final conclusion, please see for recent references [24–27].

In recent years, several works have focused on incorporating the muon ($g - 2$) from

the model-building prospects. For example, see [28–34] for minimal dark matter (DM) motivated scenarios, [35–37] for axion-like particle (ALP) motivated scenarios, [38, 39] for gauged lepton flavour models [40–66]. In leptonic model-building sectors, models in which the mediators couple exclusively to the second and third generations of leptons and are anomaly-free can exhibit attractive experimental features. Here we consider the widespread and minimal anomaly-free model based on the gauged $L_\mu - L_\tau$ symmetry [67, 68]. The gauged $U(1)_{L_\mu - L_\tau}$ introduces an additional gauge boson Z' and this new gauge boson can give an additional contribution to $(g - 2)_\mu$ via one-loop level. To keep the model consistent with current $(g - 2)_\mu$, we stick to a parameter space for Z' mass and the related gauge coupling $g_{\mu\tau}$ in the allowed region. To construct the model framework, we have introduced three heavy vector-like fermions ($N_{e,\mu,\tau}$), three right-handed Dirac neutrinos ($\nu_{(e,\mu,\tau)R}$) and two heavy scalar singlets (Φ_1, Φ_2). These fields are associated with neutrino mass generation, where light neutrino masses are generated via the Dirac SeeSaw (DSS) mechanism [17, 69–71]. We have restricted the Lagrangian to terms that do not violate lepton number by using the $U(1)_{L_\mu - L_\tau}$ symmetry.

Nevertheless, the possibility of a rich phenomenology arising from the dark sector remains open. There is strong observational evidence for dark matter (DM) from various astrophysical and cosmological observations, such as WMAP [72, 73] and Planck [4]. The rigorous search for heavy DM masses ranging from GeV still continues, yet there is no concrete signal of its existence [74]. It is theoretically plausible that new particles exist with masses far below the electroweak scale and their interactions with ordinary matter are sufficiently weak. Such feebly interacting states fall into the "dark sector" and naturally arise in many extensions of the Standard Model. The search for light DM masses in the MeV–GeV range has gained sufficient attention in recent years due to high-intensity fixed-target experiments and several low-threshold direct search experiments, which provide the most sensitive probes [75–79]. In connection with the rest of the phenomenology, we have introduced a singlet vector-like fermion, ψ , charged under the new gauge group and it behaves as a viable dark matter candidate in our study. The light Z' mediated annihilation processes allow us to consider a viable dark matter parameter region with mass in the sub-GeV scale. Such light particles (mass $< \mathcal{O}(100)$ MeV) can also decay or annihilate to the SM neutrinos and contribute to ΔN_{eff} [80–83].

This work is organized as follows: after giving a brief model description in section II, we

explore a Dirac neutrino mass model and muon ($g - 2$) constraints under the same section. Cosmological consequences are explored in section [III](#), where the fate of the RH neutrinos, dark matter and contributions to ΔN_{eff} are explored in detail in subsequent subsections. Finally, we conclude our work in section [IV](#).

II. MODEL FRAMEWORK

A. Dirac $L_\mu - L_\tau$ Model

The SM fermion content with their gauge charges under $SU(3)_c \times SU(2)_L \times U(1)_Y \times U(1)_{L_\mu - L_\tau}$ gauge symmetry are denoted as follows.

$$q_L = \begin{pmatrix} u_L \\ d_L \end{pmatrix} \sim (3, 2, \frac{1}{6}, 0), \quad u_R(d_R) \sim (3, 1, \frac{2}{3}(-\frac{1}{3}), 0)$$

$$L_e = \begin{pmatrix} \nu_e \\ e_L \end{pmatrix} \sim (1, 2, -\frac{1}{2}, 0), \quad e_R \sim (1, 1, -1, 0)$$

$$L_\mu = \begin{pmatrix} \nu_\mu \\ \mu_L \end{pmatrix} \sim (1, 2, -\frac{1}{2}, 1), \quad \mu_R \sim (1, 1, -1, 1)$$

$$L_\tau = \begin{pmatrix} \nu_\tau \\ \tau_L \end{pmatrix} \sim (1, 2, -\frac{1}{2}, -1), \quad \tau_R \sim (1, 1, -1, -1)$$

Since we want to realise Dirac neutrinos in this model, we first introduce three right handed neutrinos $\nu_{eR}, \nu_{\mu R}, \nu_{\tau R}$ singlets under the SM gauge symmetry and with $L_\mu - L_\tau$ charges $0, n_X, -n_X$ respectively. While this combination remains anomaly-free for any n_X , the importance of its value will become clear later. If $n_X = 1$, one can have a diagonal Dirac neutrino mass matrix with neutrinos coupling to the SM Higgs. Apart from the fine-tuned Yukawa required to generate sub-eV Dirac neutrino mass, such a diagonal neutrino mass matrix is also inconsistent with neutrino oscillation data [\[84\]](#), given the fact that the charged lepton mass matrix is also diagonal.

We have added three vector-like fermions (N_e, N_μ, N_τ) and two singlet scalars Φ_1 and Φ_2 with VEVs v_1 and v_2 respectively. Respective charges for the particle content are shown in Table [I](#). Apart from the Dirac neutrinos, the gauge group $U(1)_{L_\mu - L_\tau}$ introduces one

Gauge Group	Fermion		Scalar	
	$N_{(e,\mu,\tau)L}$	$\nu_{eR}, \nu_{\mu R}, \nu_{\tau R}$	Φ_1	Φ_2
$SU(2)_L$	1	1	1	1
$U(1)_Y$	0	0	0	0
$U(1)_{L_\mu - L_\tau}$	$0, 1, -1$	$0, n_X, -n_X$	$1 - n_X$	1

TABLE I: New particles and their corresponding gauge charges relevant for type I Dirac seesaw.

additional particle into the list: the new gauge boson Z' . The interaction Lagrangian with the new gauge boson Z' is given by:

$$\begin{aligned}
\mathcal{L}_{int} \supset & i\overline{N_{eL}}\gamma^\alpha D_\alpha N_{eL} + i\overline{N_{\mu L}}\gamma^\alpha D_\alpha N_{\mu L} + i\overline{N_{\tau L}}\gamma^\alpha D_\alpha N_{\tau L} \\
& + i\overline{\nu_{eR}}\gamma^\alpha D_\alpha \nu_{eR} + i\overline{\nu_{\mu R}}\gamma^\alpha D_\alpha \nu_{\mu R} + i\overline{\nu_{\tau R}}\gamma^\alpha D_\alpha \nu_{\tau R} \\
& + (D_\alpha \Phi_1)^\dagger (D^\alpha \Phi_1) + (D_\alpha \Phi_2)^\dagger (D^\alpha \Phi_2) - \frac{1}{4} Z'^{\alpha\beta} Z'_{\alpha\beta} \\
& + \frac{\epsilon}{4} Z'^{\alpha\beta} F_{\alpha\beta} + Z'_\alpha g_{\mu\tau} J^\alpha_{\mu\tau}
\end{aligned} \tag{2}$$

Here, $D_\alpha = \partial_\alpha + iq_f g_{\mu\tau} Z'_\alpha$ is the covariant derivative with q_f being the $U(1)_{L_\mu - L_\tau}$ charge for the respective particle. The $\mu - \tau$ current from eq. (2) is expressed as:

$$J_{\mu-\tau}^\alpha = q_f (\bar{\mu} \gamma^\alpha \mu + \bar{\nu}_\mu \gamma^\alpha P_L \nu_\mu - \bar{\tau} \gamma^\alpha \tau - \bar{\nu}_\tau \gamma^\alpha P_L \nu_\tau).$$

In eq. (2), $Z'_{\alpha\beta} = (\partial_\alpha Z'_\beta - \partial_\beta Z'_\alpha)$ and $F_{\alpha\beta}$ are the field strength tensors of $U(1)_{L_\mu - L_\tau}$ and $U(1)_Y$ symmetry groups respectively with kinetic mixing parameter ϵ . Even if this kinetic mixing is considered absent in the Lagrangian, it can arise at one loop level with particles charged under both the gauge sector in the loop and this mixing can be approximated to $\epsilon \simeq g_{\mu\tau}/70$ [85]. While the phenomenology of muon ($g - 2$), and DM relic in our model is not dependent on this mixing, the kinetic mixing will be tiny for our chosen parameter space. The VEVs of the singlet scalars are associated with the fate of the additional gauge boson that appears due to the $U(1)_{L_\mu - L_\tau}$ symmetry, and the new gauge boson mass can be found to be $M_{Z'} = g_{\mu\tau} \sqrt{(1 - n_X)^2 v_1^2 + v_2^2}$ with $g_{\mu\tau}$ being the $L_\mu - L_\tau$ gauge coupling.

B. Neutrino mass

While there are several ways to realise sub-eV Dirac neutrino mass, we consider the simplest possibility of type-I seesaw for Dirac neutrinos in $L_\mu - L_\tau$ model. The additional particle content required to implement type-I Dirac seesaw is shown in table I. The relevant Lagrangian is:

$$\begin{aligned} -\mathcal{L}_Y \supset & Y_e \overline{L}_e \tilde{H} N_{eR} + Y_\mu \overline{L}_\mu \tilde{H} N_{\mu R} + Y_\tau \overline{L}_\tau \tilde{H} N_{\tau R} \\ & + M_1 \overline{N}_{eL} \nu_{eR} + Y_{22} \overline{N}_{\mu L} \nu_{\mu R} \Phi_1 + Y_{33} \overline{N}_{\tau L} \nu_{\tau R} \Phi_1^\dagger \\ & + Y_{12} \overline{N}_{eL} N_{\mu R} \Phi_2^\dagger + Y_{13} \overline{N}_{eL} N_{\tau R} \Phi_2 + M_{R\alpha} \overline{N}_{\alpha L} N_{\alpha R} + \text{h.c.} \end{aligned} \quad (3)$$

We also assume a global, unbroken lepton-number symmetry to ensure that Majorana mass terms for singlet fermions are absent¹.

In $(\overline{\nu}_{\alpha L}, \overline{N}_{\alpha L})$ and $(\nu_{\alpha R}, N_{\alpha R})^T$ basis (where $\alpha = e, \mu, \tau$), the 6×6 mass matrix for light neutrinos and heavy fermions can be written as,

$$\begin{pmatrix} \overline{\nu}_{\alpha L} & \overline{N}_{\alpha L} \end{pmatrix} \begin{pmatrix} 0 & M'_D \\ M_D & M_{LR} \end{pmatrix} \begin{pmatrix} \nu_{\alpha R} \\ N_{\alpha R} \end{pmatrix}, \quad (4)$$

where

$$\begin{aligned} M'_D &= \frac{v_h}{\sqrt{2}} \begin{pmatrix} Y_e & 0 & 0 \\ 0 & Y_\mu & 0 \\ 0 & 0 & Y_\tau \end{pmatrix}, \quad M_D = \frac{v_1}{\sqrt{2}} \begin{pmatrix} \frac{\sqrt{2}M_1}{v_1} & 0 & 0 \\ 0 & Y_{22} & 0 \\ 0 & 0 & Y_{33} \end{pmatrix}, \\ M_{LR} &= \begin{pmatrix} M_{Re} & Y_{12} \frac{v_2}{\sqrt{2}} & Y_{13} \frac{v_2}{\sqrt{2}} \\ Y_{21} \frac{v_2}{\sqrt{2}} & M_{R\mu} & 0 \\ Y_{31} \frac{v_2}{\sqrt{2}} & 0 & M_{R\tau} \end{pmatrix}. \end{aligned} \quad (5)$$

Here $v_h, v_{1,2}$ are the vacuum expectation values (VEV) of the SM Higgs and two singlet scalars, respectively. The M_{LR} mass term arise due to Φ_2 being naturally larger, which allows us to have light neutrino mass within the allowed range. Therefore, working within the limit $M_D, M'_D \ll M_{LR}$, the light neutrino mass matrix is given by

$$m_\nu = -M'_D M_{LR}^{-1} M_D. \quad (6)$$

¹ Additionally, there can be direct coupling of L_e and ν_{eR} via the SM Higgs, which we are ignoring. While this term contributes only to the overall neutrino mass, additional discrete symmetries can be introduced to forbid it.

Clearly, the model predicts a diagonal charged lepton mass matrix² M_ℓ and diagonal Dirac Yukawa of light neutrinos. Thus, the non-trivial neutrino mixing will arise from the structure of M_{LR} matrix only, which is generated by the chosen scalar singlet fields. In an obvious way, there will be mixing among the heavy and light states, which gives rise to the new right-handed states as,

$$\nu_{iR} = \cos \theta_v \nu_{\alpha R} + \sin \theta_v N_{\alpha R} \quad (7)$$

$$\text{and} \quad N_{iR} = \cos \theta_v N_{\alpha R} - \sin \theta_v \nu_{\alpha R}, \quad (8)$$

where, $i = 1, 2, 3$, $\alpha = e, \mu, \tau$ and $\theta_v \sim \tan^{-1}(M_D \cdot M_{LR}^{-1})$, which will be heavily suppressed due to the large M_{LR} mass and light M_D mass. Therefore, we can safely use the notation ν_R instead of ν_{iR} in the following sections. The heavy fields associated with neutrino mass generation decay and end much earlier due to their large masses, so they wouldn't affect the latter part of the study. We keep the notation ν_{eR} for the 1st generation of right-handed neutrino and use $\nu_{\beta R}$ with $\beta = \mu, \tau$ for the rest which are having non-zero $U(1)_{L_\mu - L_\tau}$ charge.

C. Anomalous Muon Magnetic Moment

The magnetic moment of muon is given by

$$\vec{\mu}_\mu = g_\mu \left(\frac{q}{2m} \right) \vec{S}, \quad (9)$$

where, g_μ is the gyromagnetic ratio and its value is 2 for a structureless, spin $\frac{1}{2}$ particle of mass m and charge q . Any radiative correction, which couples the muon spin to the virtual fields, contributes to its magnetic moment and is given by

$$a_\mu = \frac{1}{2}(g_\mu - 2) \quad (10)$$

The anomalous muon magnetic moment has been measured very precisely, while it has also been predicted in the SM to great accuracy. In our model, the additional contribution to the muon magnetic moment comes from a one-loop diagram mediated by the Z' boson, shown in fig. 1. The contribution is given by [86–88]

$$\Delta a_\mu = \frac{\alpha'}{2\pi} \int_0^1 dx \frac{2m_\mu^2 x^2 (1-x)}{x^2 m_\mu^2 + (1-x) M_{Z'}^2} \quad (11)$$

² Yukawa interaction terms with the SM Higgs “ $\overline{L}_\alpha H \alpha_R$ ” for $\alpha = e, \mu, \tau$ are allowed and will give rise to a diagonal charged lepton mass matrix.

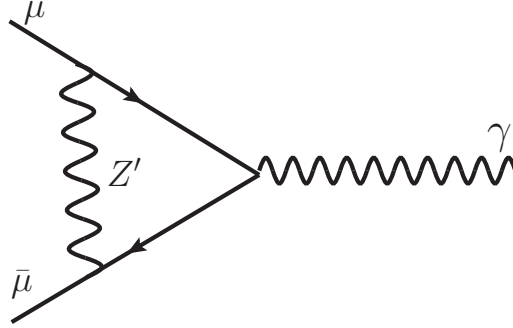


FIG. 1: Contribution to muon anomalous magnetic moment via the new gauge boson Z'

where $\alpha' = g_{\mu\tau}^2/(4\pi)$.

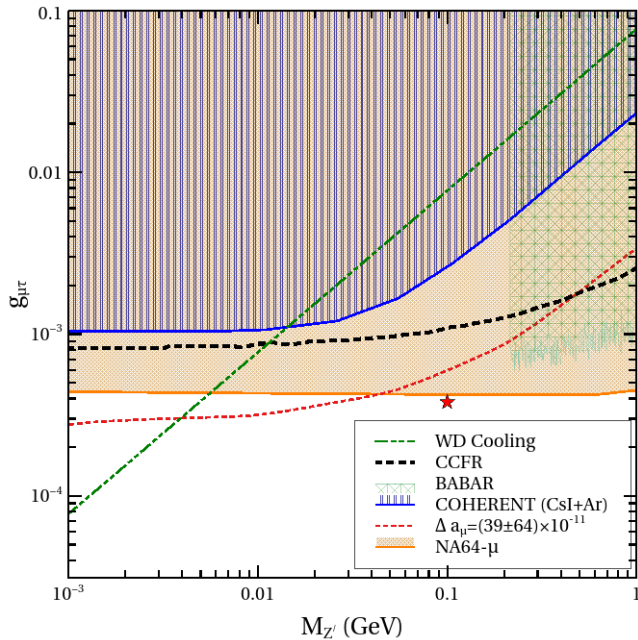


FIG. 2: Summary plot containing related bounds as indicated in the figure key. The red star is the benchmark value that we have used for further analysis.

The traditional discrepancy between the experimental value and the Standard Model prediction of the anomalous magnetic moment of the muon, a_μ , has motivated a number of new-physics interpretations. Although recent lattice-QCD-based SM predictions [23] indicate a reduced tension, the Fermilab measurement [22], when combined with updated SM inputs, remains a key probe of possible physics beyond the Standard Model. The

updated input at 1σ deviation reads as $\Delta a_\mu^{\text{exp}} = (39 \pm 64) \times 10^{-11}$. In figure 2, we have used various experimental bounds to choose a viable parameter space. The shaded grey-coloured exclusion band corresponds to the upper bound on the neutrino trident process measured by the CCFR collaboration [89]. The exclusion region labelled BABAR corresponds to the limits imposed by the BABAR collaboration [90] on four-muon final states at high Z' mass, shaded in light green. The astrophysical bounds from the cooling of the white dwarf (WD) [91, 92] exclude the upper left triangular region. The observation of coherent elastic neutrino-nucleus cross section in combined liquid argon (LAr) and caesium-iodide (CsI) performed by the COHERENT Collaboration [93] is shown in a blue solid line and shades the excluded region above the blue line. The upper bound on $(g-2)_\mu$ corresponds to $\Delta a_\mu^{\text{exp}} = (39 \pm 64) \times 10^{-11}$ is shown in a red dashed line. The latest bound from NA64- μ [94] is shown in the orange line, and the upper shaded region is the excluded region. For our further analysis in this work, we have chosen the undisturbed region, below the upper bounds, where $(g-2)_\mu$ results are consistent. Therefore we fix a benchmark region under consideration that allows $M_{Z'}$ mass below 100 MeV and the coupling value at $g_{\mu\tau} = 3.8 \times 10^{-4}$.

III. COSMOLOGICAL CONSEQUENCES

A. Fate of ν_R

We have considered that ν_{eR} maintains thermal equilibrium with the heavy fields and SM contents via Yukawa interactions. The heavy fields (N_R, Φ_1, Φ_2) along with the lighter field (ν_{eR}) leave the thermal equilibrium at a very high temperature and freeze out. The t -channel processes, such that $\nu_{eR}\nu_{eR} \leftrightarrow N_L N_L$ via Φ_2 and $\nu_{eR}\nu_{eR} \leftrightarrow \Phi_2\Phi_2$ via N_L processes will ensure the decoupling of the fields by comparing the interaction rate ($\langle \Gamma_{xx \rightarrow yy} \rangle \times n_{\text{target}}^{eq}$) with the Hubble rate. The Hubble rate varies as $H \propto \frac{T^2}{M_{\text{Planck}}}$ and n_{target}^{eq} is the equilibrium number density of the target particle. We have considered $M_N \sim \mathcal{O}(10^4)$ GeV, $M_{\Phi_1} \sim \mathcal{O}(10^2)$ GeV and $Y_{22} = Y_{33} \sim \mathcal{O}(10^{-3})$ ³ to check the decoupling profile of N_R, Φ_1 and ν_R , which are shown in Fig. 3. We can see that the light ν_{eR} decouples much earlier than the electroweak (EW) scale. Since ν_{eR} are very light, they will contribute to radiation density, hence there will be a non-zero contribution to ΔN_{eff} . Dirac neutrinos decoupling above the EW scale

³ These choices of numerical values are consistent with neutrino oscillation data.

give a fixed contribution of $\Delta N_{\text{eff}} = 0.0466 (= 0.14/3)$ [12], which is allowed from the current Planck 2018 bound [4].

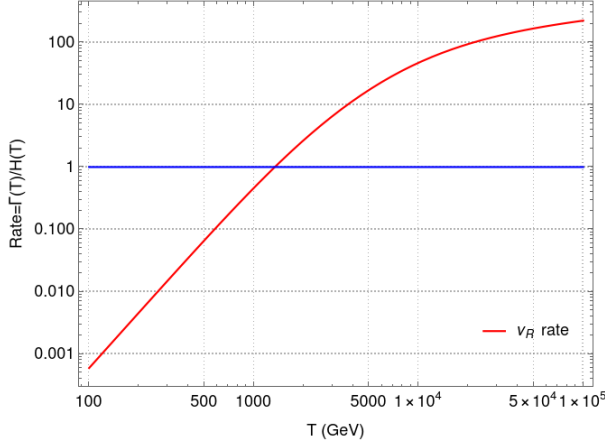


FIG. 3: Interaction rate *vs.* temperature for the light ν_{eR} . The horizontal line indicates $\Gamma/H = 1$.

As $\nu_{\beta R}$'s carry non-zero gauge charge, they may maintain thermal equilibrium with the SM plasma via gauge-mediated interactions as long as the interaction rate exceeds the Hubble expansion rate of our universe at a specific temperature. Interestingly, our choice of Z' mass will spoil the whole study if $\nu_{\beta R}$ enters thermal equilibrium with the Z' and decouples much later. The $\nu_{\beta R}$ enters the thermal equilibrium at $T \sim M_{Z'}$ and decouples later around $T \sim M_{Z'}/10$ [95]. Decoupling of light ν_R below 200 MeV will increase the ΔN_{eff} value significantly, which is strictly ruled out by Planck 2018 data [4]. The Z' mediated $\nu_R \bar{\nu}_R \leftrightarrow f \bar{f}$ interaction cross-section is evaluated as:

$$\sigma(\nu_R \bar{\nu}_R \rightarrow f \bar{f}) = \frac{k_f n_X^2 q_f^2 g_{\mu\tau}^4 \sqrt{1 - \frac{4M_f^2}{s}(2M_f^2 + s)}}{12\pi(M_{Z'}^2 - s)^2}. \quad (12)$$

Here k_f is the phase space factor, $n_X(q_f)$ is the new gauge charge for $\nu_{\beta R}(l_\alpha)$. We can see from Eq. (12), the cross-section is proportional to the gauge coupling, gauge charge and Z' mass. We have considered the parameter space as $1\text{MeV} \leq M_{Z'} \leq 200 \text{ MeV}$ and the gauge coupling $g_{\mu\tau} = 3.8 \times 10^{-4}$. To make sure that $\nu_{\beta R}$ does not enter the thermal equilibrium with Z' and spoil the study, we can tune the gauge charge n_X in such a way that $\nu_{\beta R}$ never reaches thermal equilibrium with the SM bath. In Fig. 4, we show the rate (interaction rate divided by Hubble rate) *vs.* temperature for three benchmark values of Z' mass and gauge charge n_X with fixed gauge coupling $g_{\mu\tau}$. For a gauge charge, $n_X < \mathcal{O}(10^{-6})$, the light $\nu_{\beta R}$ never reaches thermal equilibrium for our choice of parameter space and never contributes

to ΔN_{eff} via the Z' mediated s -channel process. However, such light Z' can also decay to active neutrinos and contribute independently to N_{eff} value. We will discuss it in a later section.

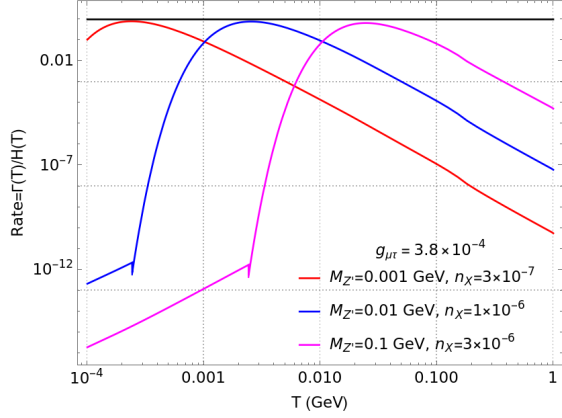


FIG. 4: Interaction rate *vs.* temperature for the new gauge boson mass $M_{Z'}$ and gauge charge, n_X with fixed $g_{\mu\tau}$. The black horizontal line represents $\Gamma/H = 1$. Hence, the region below this line indicates processes that never reach the thermal bath.

B. Dark Matter and Relic Abundance

For the dark matter sector, we introduce one additional vector-like fermion ψ with $L_\mu - L_\tau$ gauge coupling being g_ψ . The relevant Lagrangian can be written as follows:

$$\mathcal{L} \supseteq \bar{\psi} i\gamma^\mu D_\mu \psi - M_\psi \bar{\psi} \psi \quad (13)$$

Here $D_\mu \psi = (\partial_\mu + ig_\psi Z'_\mu)\psi$ and $g_\psi = n_\psi g_{\mu\tau}$ with n_ψ being gauge charge of a vector-like fermion ψ . Since n_ψ can be chosen independently, we keep g_ψ as a free parameter. We have set a benchmark point for Z' mass and coupling, consistent with $(g-2)_\mu$ results with $M_{Z'} = 100$ MeV and $g_{\mu\tau} = 3.8 \times 10^{-4}$ to divide the parameter space into two distinct regions.

For $M_{DM} > M_{Z'}$, the relevant annihilation cross section scales as the combination $g_{\mu\tau}^4/M_{DM}^2$ (for a fixed choice of gauge charges). Hence, the correct relic density depends on the gauge coupling and DM mass. On the other hand, for $M_{DM} < M_{Z'}$ the cross-section scales as the combination $g_{\mu\tau}^4 M_{DM}^2/M_{Z'}^4$, and thus the right relic density selects a value for the ratio $g_{\mu\tau}/M_{Z'}$, for a given value of DM mass. In the second case, we particularly focus

on the resonant region, where $M_{DM} \sim M_{Z'}/2$ to obtain the correct relic density. The study will increase the predictability of the model as we stick with light Z' which will be associated with current experimental constraints such as muon $(g - 2)$. They are discussed in detail below.

- When $M_{DM} > M_{Z'}$:

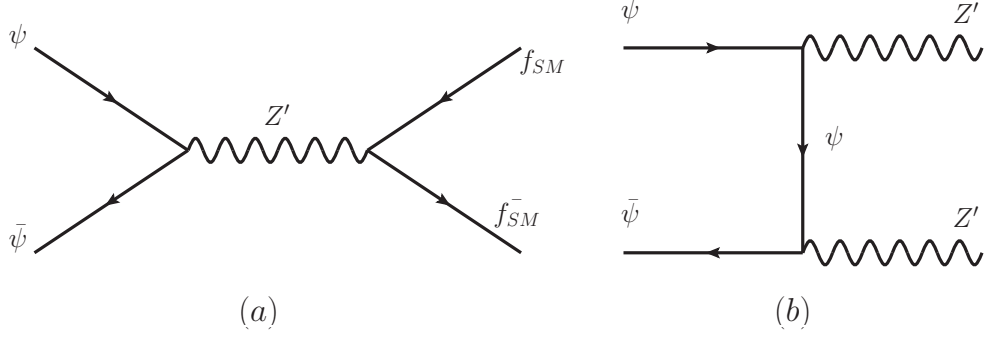


FIG. 5: Dominant contribution to the dark matter annihilation processes via Z'

The s -channel contribution to the DM annihilations are given by [96]:

$$\langle\sigma v\rangle(\psi\bar{\psi} \rightarrow f\bar{f}) = q_f^2 \frac{n_\psi^2 g_{\mu\tau}^4}{2\pi} \sqrt{1 - \frac{m_f^2}{M_\psi^2} \frac{2M_\psi^2 + m_f^2}{(4M_\psi^2 - M_{Z'}^2)^2}} \quad (14)$$

$$\langle\sigma v\rangle(\psi\bar{\psi} \rightarrow \nu\bar{\nu}) = q_f^2 \frac{n_\psi^2 g_{\mu\tau}^4}{2\pi} \frac{M_\psi^2}{(4M_\psi^2 - M_{Z'}^2)^2} \quad (15)$$

At the same time, the t -channel contribution is given by [96]:

$$\langle\sigma v\rangle(\psi\bar{\psi} \rightarrow Z'Z') = \frac{g_\psi^4}{16\pi M_\psi^2} \left(1 - \frac{M_{Z'}^2}{M_\psi^2}\right)^{3/2} \left(1 - \frac{M_{Z'}^2}{2M_\psi^2}\right)^{-2} \quad (16)$$

In the above expressions of thermal averaged cross-section, q_f stands for the lepton charge under the $U(1)_{L_\mu - L_\tau}$ symmetry and $g_\psi = n_\psi g_{\mu\tau}$. The dominant contribution to the DM relic is coming from the s -channel processes. Finally, the total contribution to the thermally averaged cross-section is given by the sum of all three contributions as:

$$\langle\sigma v\rangle = \langle\sigma v\rangle(\psi\bar{\psi} \rightarrow f\bar{f}) + \langle\sigma v\rangle(\psi\bar{\psi} \rightarrow \nu\bar{\nu}) + \langle\sigma v\rangle(\psi\bar{\psi} \rightarrow Z'Z') \quad (17)$$

The Boltzmann equation for the DM candidate for $n_{DM} = n_{\overline{DM}}$ with $n = n_{DM} + n_{\overline{DM}}$

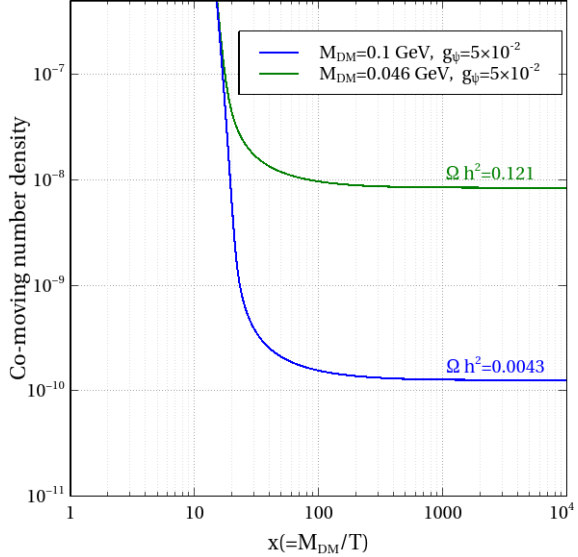


FIG. 6: Comoving number density for the DM candidate with two benchmark parameters.

can be expressed as:

$$\frac{dn}{dt} + 3nH = -\frac{1}{2}\langle\sigma v\rangle(n^2 - n_{eq}^2). \quad (18)$$

In the thermal freeze-out case, the DM particles were initially maintaining thermal equilibrium with the SM fluid via $2 \leftrightarrow 2$ scattering processes and after the freeze-out temperature T_F , they can no longer annihilate and the amount of relic abundance is given by:

$$\Omega h^2 = \frac{1.04 \times 10^9 x_F}{\sqrt{g_*} M_{\text{Pl}} \langle\sigma v\rangle} \text{GeV}^{-1}, \quad (19)$$

with $x_F = \frac{M_\psi}{T_F}$, $M_{\text{Pl}} = 1.22 \times 10^{18}$ GeV being the reduced Planck mass, g_* being the relativistic degree of freedom, and H being the Hubble parameter.

The comoving number density for the DM is shown for various input parameters in Fig. 6. The green line corresponds to $M_{DM} = 0.046$ GeV, which is close to the resonance region, triggering a sudden rise in the comoving number density (compared to the other two benchmark values) and giving rise to a relic abundance in the exact ballpark.

- **When $M_{DM} < M_{Z'}$:**

We now check the region where dark matter mass is less than the Z' mass. When DM is lighter than the Z' boson, then the $Z' \rightarrow \psi\bar{\psi}$ decay channels will contribute to the

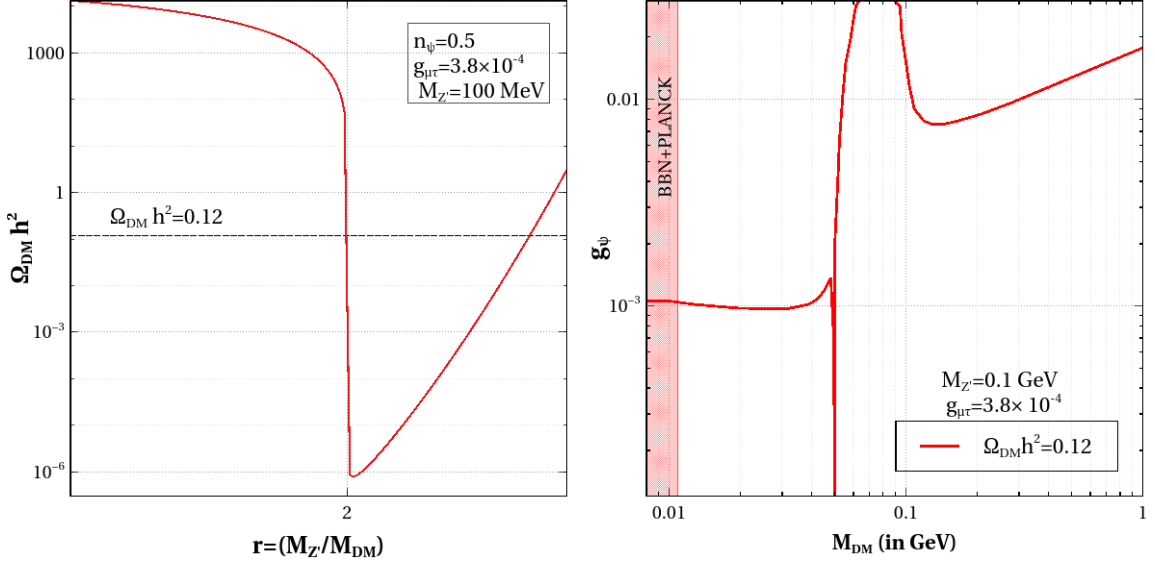


FIG. 7: (*Left*): Variation of DM relic with the mass ratio for a chosen benchmark point. Due to the resonance effect, there are two intersecting points in the dashed horizontal line. (*Right*): A red solid contour curve satisfying $\Omega_{\text{DM}} h^2 = 0.12$ in the gauge coupling (g_{ψ}) *vs.* dark matter mass (M_{DM}) plane for the benchmark point. The vertical shaded region is from the BBN+PLANCK bound on the Dirac DM candidate [99].

total annihilation cross-section. The partial decay width $Z' \rightarrow f\bar{f}$ is given by:

$$\Gamma_{Z' \rightarrow f\bar{f}} = k_f \frac{q_f^2 g_{\mu\tau}^2 M_{Z'}}{12\pi} \left(1 + 2 \frac{M_f^2}{M_{Z'}^2}\right) \sqrt{1 - \frac{4M_f^2}{M_{Z'}^2}},$$

with $k_f = 1/2$ for neutrinos, else $k_f = 1$ for other fermions⁴, q_f is the $U(1)_{L_\mu - L_\tau}$ charge for the respective fermions. Now, the Z' mediated s -channel cross-section for the $\psi\bar{\psi} \rightarrow f\bar{f}$ processes is given by [97]:

$$\sigma(s) = \sigma_f \frac{n_{\psi}^2 q_f^2 k_f g_{\mu\tau}^4 \beta_f}{12\pi s \beta_{\psi}} \left[\frac{(s + 2M_{\psi}^2)(s + 2M_f^2)}{(s - M_{Z'}^2)^2 + M_{Z'}^2 \Gamma_{Z'}^2} \right], \quad (20)$$

where s is the Mandelstam variable, $\beta_i = \sqrt{1 - 4M_i^2/s}$ and $\Gamma_{Z'} = \Gamma_{Z' \rightarrow f\bar{f}} + \Gamma_{Z' \rightarrow \psi\bar{\psi}}$ with $f = \mu, \tau, \nu_{\mu, \tau}$ ⁵. For our convenience, we have defined a parameter r as the ratio of the Z' mass to the dark matter mass, *i.e.*, $r = M_{Z'}/M_{\psi}$. The thermal-averaged

⁴ $k_f = \frac{1}{n!}$ is the phase space factor, which is multiplied to the decay width where there are n identical particles in the final state.

⁵ In this case, Z' decay to only neutrinos will be possible due to the choice of Z' mass ($\sim 0.1 \text{ GeV}$).

cross-section has been evaluated following the approach of [98] and by solving the same Boltzmann equation from eq. (18), we numerically determine the DM relic as a function of $r (= M_{Z'}/M_\psi)$.

In the first figure of Fig. 7, we show the dark matter relic abundance as a function of the mass ratio $r (= \frac{M_{Z'}}{M_\psi})$. We fixed the Z' boson mass, coupling and gauge charge here to evaluate the relic evaluation pattern. The black dotted line gives $\Omega_{DM}h^2 = 0.12$, and the red contour line shows the variation of DM relic abundance as a function of r . We can find that the red contour line crosses the dotted line on the DM relic abundance at two points. At $r \sim 2$, the DM annihilation cross-section increases abruptly due to the Breit-Wigner enhancement [100], resulting in a sudden dip in the relic abundance pattern. After hitting the resonance dip, it increases slowly due to active decay channels present in the system and crosses the horizontal line at $r \sim 2.71$.

In the second Fig. 7, we have shown a contour line and a region satisfying the current best-fit value for DM $\Omega h^2 = 0.12$ in the gauge coupling (g_ψ) vs. DM mass (M_{DM}) plane for the chosen benchmark value and the region from the summary plot. A discontinuity in the pattern is observed exactly near $M_{DM} = 50$ MeV, due to resonance and the kink around $M_{DM} \sim 100$ MeV appears as muons in the final state start contributing to the DM annihilation processes.

It is to be noticed that when such a light DM candidate is in thermal equilibrium during BBN, it can annihilate into the electron-positron pair, giving rise to an unacceptably large contribution to the expansion rate of the Universe, which severely affects the primordial element abundances measured today. Apart from this, CMB measurements also set a tight constraint on light DM entropy transferred into electrons after neutrinos decouple. The combined results from BBN+PLANCK put a lower bound on light Dirac DM mass up to $M_{DM} > 10.9$ MeV [99], which is shaded with the vertical light-red coloured band. If DM mass is larger than the muon mass (in the earlier case, when $M_{DM} > M_{Z'}$), they can dominantly annihilate into muons; however, in such a case, there is a lower bound on sub-GeV DM, which is completely ruled out for $M_{DM} < M_\mu$.

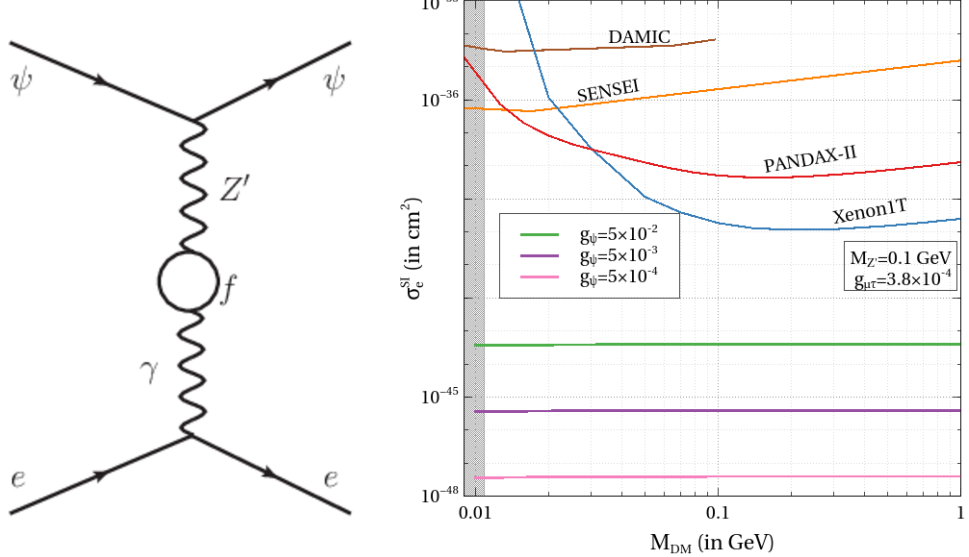


FIG. 8: (Left) DM-electron elastic scattering via one loop kinetic mixing between Z' and the photon via $f = \mu, \tau$. (Right) Variation of spin-independent elastic scattering cross-section for $\psi e \rightarrow \psi e$ process with DM mass. The vertical grey shaded region is the BBN+PLANCK bound on the Dirac DM candidate, restricting $M_{\text{DM}} < 10.9 \text{ MeV}$ [99]. We show existing experimental constraint on spin-independent $DM - e$ scattering cross-sections from DAMIC [101], SENSEI [102], PANDAX-II [103] and XENON1T [104]

1. Direct Detection of DM:

In the chosen mass range of interest throughout this study, the DM candidate does not couple directly to quarks but can have kinetic mixing between Z' and the photons via $U(1)_{L_\mu - L_\tau}$ charged fermions as shown in the left panel of Fig. 8.

Therefore, the DM-electron elastic scattering cross-section is given by [105, 106]:

$$\sigma(\psi e \rightarrow \psi e) = \frac{\mu_e^2}{\pi} \left[\frac{g_\psi \epsilon e}{(M_{Z'}^2 + \alpha_{EM} m_e^2)} \right]^2; \quad (21)$$

where μ_e is the $\psi - e$ reduced mass and $\epsilon \simeq -\frac{g_{\mu\tau}}{70}$ is the strength of the kinetic mixing.

We show the variation of the spin-independent cross-section with DM mass from Fig. 8 for three benchmark g_ψ values. This obvious suppression of cross-section values is due to the factor $m_e/M_{Z'} \ll 1$.

C. Contribution to ΔN_{eff} from the decay of light species:

For the situation where $M_{DM} < M_{Z'}$, (where we set the benchmark value of $M_{Z'} = 100$ MeV), the DM and the Z' can transfer their entropy to the neutrinos after decoupling from the bath. Interestingly, if they (DM & Z') can dump their entropy after the neutrinos decouple from the photons ($T_{\nu}^{Dec} \sim 2.3$ MeV), they can influence the Big Bang Nucleosynthesis (BBN) by triggering the Hubble expansion rate of the Universe. In this part of the work, we will primarily focus on the impact of the new Z' boson and the DM (ψ) on the neutrino energy density, which is generally parameterized by N_{eff} . The contribution from dark matter annihilation and Z' decay to N_{eff} via radiation density is given by [105]:

$$N_{\text{eff}} = N_{\nu} \left[1 + \frac{1}{N_{\nu}} \sum_{i=\psi, Z'} \frac{g_i}{2} I\left(\frac{M_i}{T_{\nu, D}}\right) \right]^{4/3}, \quad (22)$$

where, g_i is the relativistic degrees of freedom for respective particles and the function $I(x)$ describes the entropy carried by the specific particle at neutrino decoupling temperature, which is then transferred to the neutrinos. This is defined as [107]:

$$I(x) = \frac{30}{7\pi^4} \int_x^{\infty} dy \frac{(4y^2 - x^2)\sqrt{y^2 - x^2}}{e^y \pm 1}; \quad (23)$$

the $+$ ($-$) sign refers to fermion (boson) statistics.

We used the general definition $\Delta N_{\text{eff}} = N_{\text{eff}} - N_{\text{eff}}^{\text{SM}}$ to see the variation with our choice of parameters in this model. The current upper bound from Planck-2018 results restricts $\Delta N_{\text{eff}} \leq 0.285$. The combined results from SPT-3G and CMB-S4 restrict this value upto $\Delta N_{\text{eff}} \leq 0.06$.

In the left panel of Fig. 9, ΔN_{eff} as a function of $M_{Z'}$ is shown for three different production processes. The red curve shows the contribution from Z' alone, while the green and blue curves consider the DM annihilation for $r \sim 2$ and 2.71, respectively along with the Z' contributions. From this figure, we can see that if only Z' decay is producing neutrinos after they leave the thermal bath, then $M_{Z'} \leq 10.1$ MeV are ruled out by Planck 2018 data, and if light DM is also involved in the same process, then this mass bound is further stretched towards the larger value. This enhancement to ΔN_{eff} value is due to the presence of additional light DOFs, which will be there in the bath for a longer time and continue to contribute to the total energy density. In the right panel of Fig. 9, we draw two iso-contours satisfying the two bounds of ΔN_{eff} in the $M_{Z'} vs. M_{\psi}$ plane. The red-blue mesh

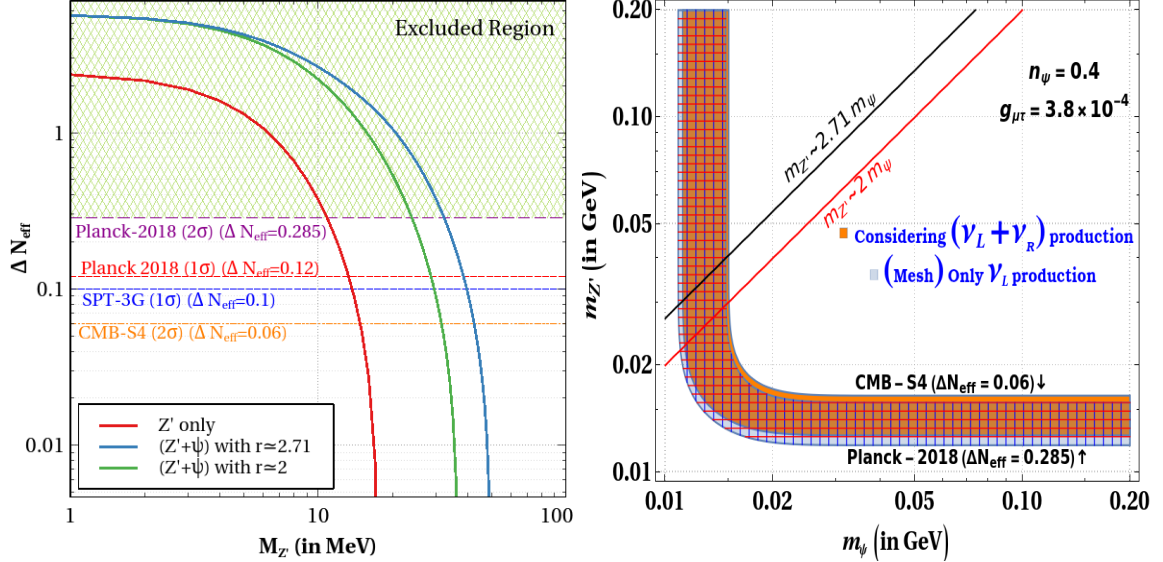


FIG. 9: (Left): Variation of ΔN_{eff} with Z' mass for three possible cases with Z' decay only (red) and $\psi\bar{\psi}$ annihilation with $r = 2.71$ (blue) and $r = 2$ (green). The horizontal lines are the related bounds as shown in the key. (Right) Comparison of ΔN_{eff} production by the active neutrinos (ν_L) only and the combination of active (ν_L) + RH neutrinos (ν_R). The contours represent the current bounds on ΔN_{eff} and the two solid lines show two mass values satisfying the DM relic of $\Omega_{\text{DM}}h^2 = 0.12$.

region represents contributions only from the SM neutrino production, while the orange region represents the production of SM neutrinos and RH neutrinos from the decay as well as annihilation processes. The two solid lines (black and red) represent the region satisfying the thermal DM relic of $\Omega_{\text{DM}}h^2 = 0.12$ for $r = \frac{M_{Z'}}{M_\psi} \sim 2.71$ and 2, respectively.

As discussed earlier, we have an additional contribution of $\Delta N_{\text{eff}} = 0.0466$ from the light ν_{eR} decoupling. Now, from the decay and annihilation of Z' and DM particle, we have new contributions to ΔN_{eff} value. The total effective ΔN_{eff} value will be the sum of the contributions arising from all the sources.

IV. CONCLUSION

We have studied a Dirac seesaw framework with the local $U(1)_{L_\mu-L_\tau}$ gauged symmetry, where the new gauge boson Z' and the corresponding gauge coupling $g_{\mu\tau}$ play key roles throughout our study. In a chronological manner, we first set up a workable Dirac neutrino

mass model. Then we choose our desired parameter space from the recent experiments, constraining the $Z' - g_{\mu\tau}$ region. The region under study is within the range of $M_{Z'} = [1, 200]$ MeV with a fixed coupling strength of $g_{\mu\tau} = 3.8 \times 10^{-4}$. Among the model ingredients, the heavy particles decay and leave the thermal bath along with the ν_{eR} , while the other two light right-handed Dirac neutrinos ($\nu_{(\mu,\tau)R}$) stay in the thermal bath for a sufficiently long period of time. Due to their specific gauge charge, they couple with the Z' and hence their cosmological consequences are studied in detail.

In the DM study, we divide the sector into two parts by the Z' mass (at 100 GeV), which is consistent with the latest $(g-2)_\mu$ result. Dark matter parameters consistent with the current best-fit value of the relic density ($\Omega_{\text{DM}} h^2$) are obtained in both regions, primarily focusing near the resonance region ($\sim \frac{M_{Z'}}{2}$). The additional contributions to N_{eff} are calculated via all the possible processes that can contribute to the radiation density. We show the contributions coming from the RH neutrinos ($\nu_{\mu R}$ and $\nu_{\tau R}$) having the non-zero $U(1)_{L_\mu - L_\tau}$ only. The ν_{eR} will leave the thermal bath at a very early time (before the EWSB) and it will give a fixed contribution of $\Delta N_{\text{eff}} = 0.0466$. The final value of ΔN_{eff} will be the combined contributions of all possibilities. We also show the connections between the mass of DM and the mass of Z' from ΔN_{eff} constraints, which come from the production of SM neutrinos or the $(\text{SM} + \nu_R)$ neutrinos. To keep on the safe side, we check the spin-independent $DM - electron$ scattering cross-section, as such, light DM masses will be sensitive only to them, which remains suppressed due to the factor $m_e/M_{Z'} \ll 1$.

V. ACKNOWLEDGEMENTS

The author thanks Debasish Borah (IIT-Guwahati) for suggesting the original idea of this work. Various aspects of this research were discussed with Arunansu Sil (IIT-Guwahati) and Debasish Borah (IIT-Guwahati), and the author is grateful to them for insightful discussions. The author also sincerely thanks Satyabrata Mahapatra (IIT-Goa) for carefully reading & reviewing the manuscript and providing valuable comments and suggestions that improved the presentation of this work. The author acknowledges Devabrat Mahanta (Pragjyotish College) for discussions on various aspects of this work.

[1] G. Mangano, G. Miele, S. Pastor, T. Pinto, O. Pisanti, and P. D. Serpico, *Relic neutrino decoupling including flavor oscillations*, *Nucl. Phys. B* **729** (2005) 221–234, [[hep-ph/0506164](#)].

[2] E. Grohs, G. M. Fuller, C. T. Kishimoto, M. W. Paris, and A. Vlasenko, *Neutrino energy transport in weak decoupling and big bang nucleosynthesis*, *Phys. Rev. D* **93** (2016), no. 8 083522, [[arXiv:1512.02205](#)].

[3] P. F. de Salas and S. Pastor, *Relic neutrino decoupling with flavour oscillations revisited*, *JCAP* **1607** (2016), no. 07 051, [[arXiv:1606.06986](#)].

[4] **Planck** Collaboration, N. Aghanim *et al.*, *Planck 2018 results. VI. Cosmological parameters*, *Astron. Astrophys.* **641** (2020) A6, [[arXiv:1807.06209](#)]. [Erratum: *Astron. Astrophys.* 652, C4 (2021)].

[5] R. H. Cyburt, B. D. Fields, K. A. Olive, and T.-H. Yeh, *Big Bang Nucleosynthesis: 2015*, *Rev. Mod. Phys.* **88** (2016) 015004, [[arXiv:1505.01076](#)].

[6] K. Abazajian *et al.*, *CMB-S4 Science Case, Reference Design, and Project Plan*, [[arXiv:1907.04473](#)].

[7] D. Nanda and D. Borah, *Connecting Light Dirac Neutrinos to a Multi-component Dark Matter Scenario in Gauged $B - L$ Model*, *Eur. Phys. J. C* **80** (2020), no. 6 557, [[arXiv:1911.04703](#)].

[8] S.-P. Li, X.-Q. Li, X.-S. Yan, and Y.-D. Yang, *Cosmological imprints of Dirac neutrinos in a keV-vacuum 2HDM**, *Chin. Phys. C* **47** (2023), no. 4 043109, [[arXiv:2202.10250](#)].

[9] K. N. Abazajian and J. Heeck, *Observing Dirac neutrinos in the cosmic microwave background*, *Phys. Rev. D* **100** (2019) 075027, [[arXiv:1908.03286](#)].

[10] P. Fileviez Pérez, C. Murgui, and A. D. Plascencia, *Neutrino-Dark Matter Connections in Gauge Theories*, *Phys. Rev. D* **100** (2019), no. 3 035041, [[arXiv:1905.06344](#)].

[11] C. Han, M. L. López-Ibáñez, B. Peng, and J. M. Yang, *Dirac dark matter in $U(1)_{B-L}$ with the Stueckelberg mechanism*, *Nucl. Phys. B* **959** (2020) 115154, [[arXiv:2001.04078](#)].

[12] X. Luo, W. Rodejohann, and X.-J. Xu, *Dirac neutrinos and N_{eff}* , *JCAP* **06** (2020) 058, [[arXiv:2005.01629](#)].

[13] P. Adshead, Y. Cui, A. J. Long, and M. Shamma, *Unraveling the Dirac neutrino with*

cosmological and terrestrial detectors, Phys. Lett. B **823** (2021) 136736, [[arXiv:2009.07852](#)].

[14] X. Luo, W. Rodejohann, and X.-J. Xu, *Dirac neutrinos and N_{eff} . Part II. The freeze-in case, JCAP* **03** (2021) 082, [[arXiv:2011.13059](#)].

[15] D. Mahanta and D. Borah, *Low scale Dirac leptogenesis and dark matter with observable ΔN_{eff}* , [arXiv:2101.02092](#).

[16] A. Biswas, D. Borah, and D. Nanda, *Light Dirac neutrino portal dark matter with observable ΔN_{eff} , JCAP* **10** (2021) 002, [[arXiv:2103.05648](#)].

[17] D. Borah, S. Mahapatra, D. Nanda, and N. Sahu, *Type II Dirac seesaw with observable ΔN_{eff} in the light of W -mass anomaly, Phys. Lett. B* **833** (2022) 137297, [[arXiv:2204.08266](#)].

[18] D. Borah, A. Dasgupta, C. Majumdar, and D. Nanda, *Observing left-right symmetry in the cosmic microwave background, Phys. Rev. D* **102** (2020), no. 3 035025, [[arXiv:2005.02343](#)].

[19] A. Biswas, D. K. Ghosh, and D. Nanda, *Concealing Dirac neutrinos from cosmic microwave background, JCAP* **10** (2022) 006, [[arXiv:2206.13710](#)].

[20] A. Biswas, D. Borah, N. Das, and D. Nanda, *Freeze-in dark matter via a light Dirac neutrino portal, Phys. Rev. D* **107** (2023), no. 1 015015, [[arXiv:2205.01144](#)].

[21] D. Borah, P. Das, and D. Nanda, *Observable ΔN_{eff} in Dirac scotogenic model, Eur. Phys. J. C* **84** (2024), no. 2 140, [[arXiv:2211.13168](#)].

[22] **Muon g-2** Collaboration, D. P. Aguillard *et al.*, *Measurement of the Positive Muon Anomalous Magnetic Moment to 127 ppb, Phys. Rev. Lett.* **135** (2025), no. 10 101802, [[arXiv:2506.03069](#)].

[23] R. Aliberti *et al.*, *The anomalous magnetic moment of the muon in the Standard Model: an update, Phys. Rept.* **1143** (2025) 1–158, [[arXiv:2505.21476](#)].

[24] L. Di Luzio, A. Keshavarzi, A. Masiero, and P. Paradisi, *Model-Independent Tests of the Hadronic Vacuum Polarization Contribution to the Muon g-2, Phys. Rev. Lett.* **134** (2025), no. 1 011902, [[arXiv:2408.01123](#)].

[25] D. W. Hertzog and M. Hoferichter, *The anomalous magnetic moment of the muon: status and perspectives, [arXiv:2512.16980](#)*.

[26] M. Hoferichter, J. Lüdtke, L. Naterop, M. Procura, and P. Stoffer, *Improved Evaluation of the Electroweak Contribution to Muon g-2, Phys. Rev. Lett.* **134** (2025), no. 20 201801,

[arXiv:2503.04883].

- [27] S. Kuberski, M. Cè, G. von Hippel, H. B. Meyer, K. Ottnad, A. Risch, and H. Wittig, *Hadronic vacuum polarization in the muon $g - 2$: the short-distance contribution from lattice QCD*, *JHEP* **03** (2024) 172, [arXiv:2401.11895].
- [28] G. Arcadi, L. Calibbi, M. Fedele, and F. Mescia, *Muon $g - 2$ and B-anomalies from Dark Matter*, arXiv:2104.03228.
- [29] B. Zhu and X. Liu, *Probing light dark matter with scalar mediator: muon $(g - 2)$ deviation, the proton radius puzzle*, arXiv:2104.03238.
- [30] X.-F. Han, T. Li, H.-X. Wang, L. Wang, and Y. Zhang, *Lepton-specific inert two-Higgs-doublet model confronted with the new results for muon and electron $g-2$ anomaly and multi-lepton searches at the LHC*, arXiv:2104.03227.
- [31] S. Baum, M. Carena, N. R. Shah, and C. E. M. Wagner, *The Tiny $(g-2)$ Muon Wobble from Small- μ Supersymmetry*, arXiv:2104.03302.
- [32] Y. Bai and J. Berger, *Muon $g-2$ in Lepton Portal Dark Matter*, arXiv:2104.03301.
- [33] P. Das, M. Kumar Das, and N. Khan, *The FIMP-WIMP dark matter and Muon $g-2$ in the extended singlet scalar model*, arXiv:2104.03271.
- [34] C.-T. Lu, R. Ramos, and Y.-L. Sming Tsai, *Shedding light on dark matter with recent muon $g-2$ and Higgs exotic decay measurements*, arXiv:2104.04503.
- [35] S.-F. Ge, X.-D. Ma, and P. Pasquini, *Probing the Dark Axion Portal with Muon Anomalous Magnetic Moment*, arXiv:2104.03276.
- [36] V. Brdar, S. Jana, J. Kubo, and M. Lindner, *Semi-secretly interacting ALP as an explanation of Fermilab muon $g - 2$ measurement*, arXiv:2104.03282.
- [37] M. A. Buen-Abad, J. Fan, M. Reece, and C. Sun, *Challenges for an axion explanation of the muon $g - 2$ measurement*, arXiv:2104.03267.
- [38] L. Zu, X. Pan, L. Feng, Q. Yuan, and Y.-Z. Fan, *Constraining $U(1)_{L_\mu - L_\tau}$ charged dark matter model for muon $g - 2$ anomaly with AMS-02 electron and positron data*, arXiv:2104.03340.
- [39] D. W. P. Amaral, D. G. Cerdeño, A. Cheek, and P. Foldenauer, *Distinguishing $U(1)_{L_\mu - L_\tau}$ from $U(1)_{L_\mu}$ as a solution for $(g - 2)_\mu$ with neutrinos*, arXiv:2104.03297.
- [40] M. Endo, K. Hamaguchi, S. Iwamoto, and T. Kitahara, *Supersymmetric Interpretation of the Muon $g - 2$ Anomaly*, arXiv:2104.03217.

[41] W. Ahmed, I. Khan, J. Li, T. Li, S. Raza, and W. Zhang, *The Natural Explanation of the Muon Anomalous Magnetic Moment via the Electroweak Supersymmetry from the GmSUGRA in the MSSM*, [arXiv:2104.03491](https://arxiv.org/abs/2104.03491).

[42] A. Greljo, P. Stangl, A. E. Thomsen, and J. Zupan, *On $(g - 2)_\mu$ from gauged $U(1)_X$* , *JHEP* **07** (2022) 098, [[arXiv:2203.13731](https://arxiv.org/abs/2203.13731)].

[43] M. Abdughani, Y.-Z. Fan, L. Feng, Y.-L. Sming Tsai, L. Wu, and Q. Yuan, *A common origin of muon $g-2$ anomaly, Galaxy Center GeV excess and AMS-02 anti-proton excess in the NMSSM*, [arXiv:2104.03274](https://arxiv.org/abs/2104.03274).

[44] M. Van Beekveld, W. Beenakker, M. Schutten, and J. De Wit, *Dark matter, fine-tuning and $(g - 2)_\mu$ in the pMSSM*, [arXiv:2104.03245](https://arxiv.org/abs/2104.03245).

[45] P. Cox, C. Han, and T. T. Yanagida, *Muon $g - 2$ and Co-annihilating Dark Matter in the MSSM*, [arXiv:2104.03290](https://arxiv.org/abs/2104.03290).

[46] F. Wang, L. Wu, Y. Xiao, J. M. Yang, and Y. Zhang, *GUT-scale constrained SUSY in light of E989 muon $g-2$ measurement*, [arXiv:2104.03262](https://arxiv.org/abs/2104.03262).

[47] Y. Gu, N. Liu, L. Su, and D. Wang, *Heavy Bino and Slepton for Muon $g-2$ Anomaly*, [arXiv:2104.03239](https://arxiv.org/abs/2104.03239).

[48] J. Cao, J. Lian, Y. Pan, D. Zhang, and P. Zhu, *Improved $(g - 2)_\mu$ Measurement and Singlino dark matter in the general NMSSM*, [arXiv:2104.03284](https://arxiv.org/abs/2104.03284).

[49] W. Yin, *Muon $g - 2$ Anomaly in Anomaly Mediation*, [arXiv:2104.03259](https://arxiv.org/abs/2104.03259).

[50] C. Han, *Muon $g-2$ and CP violation in MSSM*, [arXiv:2104.03292](https://arxiv.org/abs/2104.03292).

[51] A. Aboubrahim, M. Klasen, and P. Nath, *What Fermilab $(g - 2)_\mu$ experiment tells us about discovering SUSY at HL-LHC and HE-LHC*, [arXiv:2104.03839](https://arxiv.org/abs/2104.03839).

[52] J.-L. Yang, H.-B. Zhang, C.-X. Liu, X.-X. Dong, and T.-F. Feng, *Muon $(g - 2)$ in the B-LSSM*, [arXiv:2104.03542](https://arxiv.org/abs/2104.03542).

[53] M. Chakraborti, L. Roszkowski, and S. Trojanowski, *GUT-constrained supersymmetry and dark matter in light of the new $(g - 2)_\mu$ determination*, [arXiv:2104.04458](https://arxiv.org/abs/2104.04458).

[54] P. M. Ferreira, B. L. Gonçalves, F. R. Joaquim, and M. Sher, *$(g - 2)_\mu$ in the 2HDM and slightly beyond – an updated view*, [arXiv:2104.03367](https://arxiv.org/abs/2104.03367).

[55] H.-X. Wang, L. Wang, and Y. Zhang, *Revisiting the μ - τ -philic Higgs doublet in light of the muon $g - 2$ anomaly, τ decays, and multi-lepton searches at the LHC*, [arXiv:2104.03242](https://arxiv.org/abs/2104.03242).

[56] T. Li, J. Pei, and W. Zhang, *Muon Anomalous Magnetic Moment and Higgs Potential*

Stability in the 331 Model from E_6 , [arXiv:2104.03334](https://arxiv.org/abs/2104.03334).

- [57] M. Cadeddu, N. Cargioli, F. Dordei, C. Giunti, and E. Picciano, *Muon and electron $g-2$, proton and cesium weak charges implications on dark $\mathbf{Z_d}$ models*, [arXiv:2104.03280](https://arxiv.org/abs/2104.03280).
- [58] L. Calibbi, M. L. López-Ibáñez, A. Melis, and O. Vives, *Implications of the Muon $g-2$ result on the flavour structure of the lepton mass matrix*, [arXiv:2104.03296](https://arxiv.org/abs/2104.03296).
- [59] J. Chen, Q. Wen, F. Xu, and M. Zhang, *Flavor Anomalies Accommodated in A Flavor Gauged Two Higgs Doublet Model*, [arXiv:2104.03699](https://arxiv.org/abs/2104.03699).
- [60] P. Escribano, J. Terol-Calvo, and A. Vicente, *$(g-2)_{e,\mu}$ in an extended inverse type-III seesaw*, [arXiv:2104.03705](https://arxiv.org/abs/2104.03705).
- [61] E. J. Chun and T. Mondal, *Leptophilic bosons and muon $g-2$ at lepton colliders*, [arXiv:2104.03701](https://arxiv.org/abs/2104.03701).
- [62] G. Arcadi, A. S. De Jesus, T. B. De Melo, F. S. Queiroz, and Y. S. Villamizar, *A 2HDM for the $g-2$ and Dark Matter*, [arXiv:2104.04456](https://arxiv.org/abs/2104.04456).
- [63] C.-H. Chen, C.-W. Chiang, and T. Nomura, *Muon $g-2$ in two-Higgs-doublet model with type-II seesaw mechanism*, [arXiv:2104.03275](https://arxiv.org/abs/2104.03275).
- [64] T. Nomura and H. Okada, *Explanations for anomalies of muon anomalous magnetic dipole moment, $b \rightarrow s\mu\bar{\mu}$ and radiative neutrino masses in a leptoquark model*, [arXiv:2104.03248](https://arxiv.org/abs/2104.03248).
- [65] S. Mahapatra, R. N. Mohapatra, and N. Sahu, *Gauged $L_e - L_\mu - L_\tau$ symmetry, fourth generation, neutrino mass and dark matter*, *Phys. Lett. B* **843** (2023) 138011, [[arXiv:2302.01784](https://arxiv.org/abs/2302.01784)].
- [66] D. Borah, S. Mahapatra, N. Sahu, and V. S. Thounaojam, *Light thermal dark matter models in the light of DAMIC-M 2025 constraints*, *Phys. Rev. D* **113** (2026), no. 1 015026, [[arXiv:2509.16319](https://arxiv.org/abs/2509.16319)].
- [67] X. He, G. C. Joshi, H. Lew, and R. Volkas, *NEW Z-prime PHENOMENOLOGY*, *Phys. Rev. D* **43** (1991) 22–24.
- [68] X.-G. He, G. C. Joshi, H. Lew, and R. R. Volkas, *Simplest Z-prime model*, *Phys. Rev. D* **44** (1991) 2118–2132.
- [69] Z. A. Borboruah, D. Borah, L. Malhotra, and U. Patel, *Minimal Dirac seesaw dark matter*, *Phys. Rev. D* **112** (2025), no. 1 015022, [[arXiv:2412.12267](https://arxiv.org/abs/2412.12267)].
- [70] S.-P. Chen and P.-H. Gu, *Undemocratic Dirac seesaw*, *Nucl. Phys. B* **985** (2022) 116028, [[arXiv:2210.05307](https://arxiv.org/abs/2210.05307)].

[71] D. Borah and B. Karmakar, *A₄ flavour model for Dirac neutrinos: Type I and inverse seesaw*, *Phys. Lett.* **B780** (2018) 461–470, [[arXiv:1712.06407](#)].

[72] **WMAP** Collaboration, C. L. Bennett *et al.*, *Nine-Year Wilkinson Microwave Anisotropy Probe (WMAP) Observations: Final Maps and Results*, *Astrophys. J. Suppl.* **208** (2013) 20, [[arXiv:1212.5225](#)].

[73] **WMAP** Collaboration, C. L. Bennett *et al.*, *First year Wilkinson Microwave Anisotropy Probe (WMAP) observations: Preliminary maps and basic results*, *Astrophys. J. Suppl.* **148** (2003) 1–27, [[astro-ph/0302207](#)].

[74] **LZ** Collaboration, J. Aalbers *et al.*, *First Dark Matter Search Results from the LUX-ZEPLIN (LZ) Experiment*, [arXiv:2207.03764](#).

[75] J. Beacham *et al.*, *Physics Beyond Colliders at CERN: Beyond the Standard Model Working Group Report*, *J. Phys. G* **47** (2020), no. 1 010501, [[arXiv:1901.09966](#)].

[76] P. Ilten *et al.*, *Experiments and Facilities for Accelerator-Based Dark Sector Searches*, in *Snowmass 2021*, 6, 2022. [arXiv:2206.04220](#).

[77] R. Essig *et al.*, *Snowmass2021 Cosmic Frontier: The landscape of low-threshold dark matter direct detection in the next decade*, in *Snowmass 2021*, 3, 2022. [arXiv:2203.08297](#).

[78] **Particle Data Group** Collaboration, S. Navas *et al.*, *Review of particle physics*, *Phys. Rev. D* **110** (2024), no. 3 030001.

[79] P. Du, D. Egana-Ugrinovic, R. Essig, and M. Sholapurkar, *Sources of Low-Energy Events in Low-Threshold Dark-Matter and Neutrino Detectors*, *Phys. Rev. X* **12** (2022), no. 1 011009, [[arXiv:2011.13939](#)].

[80] D. Baumann, D. Green, and B. Wallisch, *Searching for light relics with large-scale structure*, *JCAP* **08** (2018) 029, [[arXiv:1712.08067](#)].

[81] M. Blennow, E. Fernandez-Martinez, O. Mena, J. Redondo, and P. Serra, *Asymmetric Dark Matter and Dark Radiation*, *JCAP* **07** (2012) 022, [[arXiv:1203.5803](#)].

[82] T.-H. Yeh, J. Shelton, K. A. Olive, and B. D. Fields, *Probing physics beyond the standard model: limits from BBN and the CMB independently and combined*, *JCAP* **10** (2022) 046, [[arXiv:2207.13133](#)].

[83] M. Breitbach, J. Kopp, E. Madge, T. Opferkuch, and P. Schwaller, *Dark, Cold, and Noisy: Constraining Secluded Hidden Sectors with Gravitational Waves*, *JCAP* **07** (2019) 007, [[arXiv:1811.11175](#)].

[84] **Particle Data Group** Collaboration, P. A. Zyla *et al.*, *Review of Particle Physics, PTEP* **2020** (2020), no. 8 083C01.

[85] M. Escudero, D. Hooper, G. Krnjaic, and M. Pierre, *Cosmology with A Very Light $L_\mu - L_\tau$ Gauge Boson*, *JHEP* **03** (2019) 071, [[arXiv:1901.02010](https://arxiv.org/abs/1901.02010)].

[86] S. J. Brodsky and E. De Rafael, *SUGGESTED BOSON - LEPTON PAIR COUPLINGS AND THE ANOMALOUS MAGNETIC MOMENT OF THE MUON*, *Phys. Rev.* **168** (1968) 1620–1622.

[87] S. Baek and P. Ko, *Phenomenology of $U(1)(L(\mu)-L(\tau))$ charged dark matter at PAMELA and colliders*, *JCAP* **10** (2009) 011, [[arXiv:0811.1646](https://arxiv.org/abs/0811.1646)].

[88] F. S. Queiroz and W. Shepherd, *New Physics Contributions to the Muon Anomalous Magnetic Moment: A Numerical Code*, *Phys. Rev. D* **89** (2014), no. 9 095024, [[arXiv:1403.2309](https://arxiv.org/abs/1403.2309)].

[89] W. Altmannshofer, S. Gori, M. Pospelov, and I. Yavin, *Neutrino Trident Production: A Powerful Probe of New Physics with Neutrino Beams*, *Phys. Rev. Lett.* **113** (2014) 091801, [[arXiv:1406.2332](https://arxiv.org/abs/1406.2332)].

[90] **BaBar** Collaboration, J. P. Lees *et al.*, *Search for a muonic dark force at BABAR*, *Phys. Rev. D* **94** (2016), no. 1 011102, [[arXiv:1606.03501](https://arxiv.org/abs/1606.03501)].

[91] M. Bauer, P. Foldenauer, and J. Jaeckel, *Hunting All the Hidden Photons*, *JHEP* **18** (2020) 094, [[arXiv:1803.05466](https://arxiv.org/abs/1803.05466)].

[92] A. Kamada, K. Kaneta, K. Yanagi, and H.-B. Yu, *Self-interacting dark matter and muon $g - 2$ in a gauged $U(1)_{L_\mu - L_\tau}$ model*, *JHEP* **06** (2018) 117, [[arXiv:1805.00651](https://arxiv.org/abs/1805.00651)].

[93] **COHERENT** Collaboration, D. Akimov *et al.*, *First Measurement of Coherent Elastic Neutrino-Nucleus Scattering on Argon*, *Phys. Rev. Lett.* **126** (2021), no. 1 012002, [[arXiv:2003.10630](https://arxiv.org/abs/2003.10630)].

[94] **NA64** Collaboration, Y. M. Andreev *et al.*, *First Results in the Search for Dark Sectors at NA64 with the CERN SPS High Energy Muon Beam*, *Phys. Rev. Lett.* **132** (2024), no. 21 211803, [[arXiv:2401.01708](https://arxiv.org/abs/2401.01708)].

[95] J. Heeck and H. Zhang, *Exotic Charges, Multicomponent Dark Matter and Light Sterile Neutrinos*, *JHEP* **05** (2013) 164, [[arXiv:1211.0538](https://arxiv.org/abs/1211.0538)].

[96] W. Altmannshofer, S. Gori, S. Profumo, and F. S. Queiroz, *Explaining dark matter and B decay anomalies with an $L_\mu - L_\tau$ model*, *JHEP* **12** (2016) 106, [[arXiv:1609.04026](https://arxiv.org/abs/1609.04026)].

[97] I. Holst, D. Hooper, and G. Krnjaic, *Simplest and Most Predictive Model of Muon $g-2$ and Thermal Dark Matter*, *Phys. Rev. Lett.* **128** (2022), no. 14 141802, [[arXiv:2107.09067](https://arxiv.org/abs/2107.09067)].

[98] P. Gondolo and G. Gelmini, *Cosmic abundances of stable particles: Improved analysis*, *Nucl. Phys.* **B360** (1991) 145–179.

[99] N. Sabti, J. Alvey, M. Escudero, M. Fairbairn, and D. Blas, *Refined Bounds on MeV-scale Thermal Dark Sectors from BBN and the CMB*, *JCAP* **01** (2020) 004, [[arXiv:1910.01649](https://arxiv.org/abs/1910.01649)].

[100] M. Ibe, H. Murayama, and T. T. Yanagida, *Breit-Wigner Enhancement of Dark Matter Annihilation*, *Phys. Rev.* **D79** (2009) 095009, [[arXiv:0812.0072](https://arxiv.org/abs/0812.0072)].

[101] **DAMIC** Collaboration, A. Aguilar-Arevalo *et al.*, *Constraints on Light Dark Matter Particles Interacting with Electrons from DAMIC at SNOLAB*, *Phys. Rev. Lett.* **123** (2019), no. 18 181802, [[arXiv:1907.12628](https://arxiv.org/abs/1907.12628)].

[102] **SENSEI** Collaboration, L. Barak *et al.*, *SENSEI: Direct-Detection Results on sub-GeV Dark Matter from a New Skipper-CCD*, *Phys. Rev. Lett.* **125** (2020), no. 17 171802, [[arXiv:2004.11378](https://arxiv.org/abs/2004.11378)].

[103] **PandaX-II** Collaboration, C. Cheng *et al.*, *Search for Light Dark Matter-Electron Scatterings in the PandaX-II Experiment*, *Phys. Rev. Lett.* **126** (2021), no. 21 211803, [[arXiv:2101.07479](https://arxiv.org/abs/2101.07479)].

[104] **XENON** Collaboration, E. Aprile *et al.*, *Light Dark Matter Search with Ionization Signals in XENON1T*, *Phys. Rev. Lett.* **123** (2019), no. 25 251801, [[arXiv:1907.11485](https://arxiv.org/abs/1907.11485)].

[105] M. Drees and W. Zhao, $U(1)_{L\mu-L\tau}$ for light dark matter, $g_\mu 2$, the 511 keV excess and the Hubble tension, *Phys. Lett. B* **827** (2022) 136948, [[arXiv:2107.14528](https://arxiv.org/abs/2107.14528)].

[106] R. Essig, M. Fernandez-Serra, J. Mardon, A. Soto, T. Volansky, and T.-T. Yu, *Direct Detection of sub-GeV Dark Matter with Semiconductor Targets*, *JHEP* **05** (2016) 046, [[arXiv:1509.01598](https://arxiv.org/abs/1509.01598)].

[107] C. Boehm, M. J. Dolan, and C. McCabe, *A Lower Bound on the Mass of Cold Thermal Dark Matter from Planck*, *JCAP* **08** (2013) 041, [[arXiv:1303.6270](https://arxiv.org/abs/1303.6270)].